research article

Combined seismic and magnetotelluric imaging of upper crystalline crust in the Southern Bohemian Massif

K. Aric[1,4], A. Adam[2] & D. K. Smythe[3]

Introduction

Combined engineering-scale seismic and magnetotelluric methods are not usually thought of as useful tools for investigating the uppermost (< 1 km deep) crystalline crust, although combined methods are making progress at the larger oil exploration scale in sedimentary basins (Nagy 1996). By 'engineering-scale' we mean those field methods which can be applied by a team of two or three persons with one or two vehicles, with equipment normally used for engineering site surveys, and with survey field costs of only a few hundred dollars per day. We report here a case history where a combination of such modest geophysical resources has been used to try to clarify some regional structural and tectonic relationships which orthodox geological mapping had failed to resolve.

The Southern Bohemian Massif in Austria is a deeply eroded remnant of the Variscan orogen of central Europe, comprising medium-grade metamorphic rocks of Precambrian to Palaeozoic age, extensively intruded by granitic plutons of Variscan age. The paper deals with the location of the boundary between two major divisions of the massif, the Moldanubian in the west and the Moravian in the east, in the neighbourhood of the Messern Arc. The geological problem is essentially whether the Moravian Bittesch Gneiss is identical to or distinct from the Moldanubian Dobra Gneiss in the west. Wieseneder *et al.* (1976) point to the remarkable similarities between the two gneiss units. The two outcrops are separated at the surface by the Variegated Sequence (Fig. 1) and by granulites and paragneisses. Fuchs & Matura (1980) suggest that the surface outcrops are linked at depth by a synclinorial (trough-shaped) structure. If the synclinorial structure is correct, it implies that the boundary between the Moldanubian and the Moravian must lie some 30 km to the west, at the western border of the Dobra Gneiss. If, on the other hand, as Thiele (1976) assumes, the Variegated Sequence and granulites have been thrust eastwards over the Bittesch Gneiss, there is no genetic relation between the two gneiss sequences. This question is the subject of our combined seismic and magnetotelluric investigations. Although our spatially very limited data turn out to be consistent with either models, we demonstrate that modest geophysical techniques can be used to image structures within crystalline basement.

[1]Institute of Meteorology and Geophysics, University of Vienna, Althanstrasse 14, A-1090 Vienna, Austria, [2]Geodetical and Geophysical Research Institute of the Hungarian Academy of Sciences, Csatka E. u. 6–8, H-9400 Sopron, Hungary, [3]Department of Geology & Applied Geology, University of Glasgow, Glasgow G12 8QQ, Scotland. [4]Correspondence

Seismic refraction and reflection profiling

Figure 1 shows the locations of the combined high-resolution refraction/reflection seismic measurements performed to resolve shallow structures down to 2 km depth. We discuss herein only the Messern profile, which is about 5 km in length, and which runs across the geological strike. It starts in the west within the granulite overlying the Dobra Gneiss of St. Leonhard in the west and runs across the Variegated Sequence, to finish within the Bittesch Gneiss unit in the east. The strike-parallel Nondorf profile (Fig. 1) is not discussed in this paper.

The 24-channel digital acquisition system used had a 72 dB dynamic range with a 2 ms sample interval. The seismic source was a vacuum-assisted weight drop (Brückl 1988) at a 10 m source interval, with 16-fold vertical stacking of weight drops at each shot-point. Geophone groups (40 m interval) consisted of 12 30 Hz geophones with an array length of 20 m. Since the recording system did not have built-in roll-along capability, a jump-roll split spread geometry was used, in which the source was moved forward through the fixed spread for 24 shots (Fig. 2). This results in asymmetrical split-spread shot files. The spread was then shifted forward to make the current shot-point near the rear of the spread again, and the process was repeated. The data were sorted as 96 trace common receiver gathers with a 10-m trace spacing, giving a balanced 12-fold CMP coverage at a 5-m interval, but with a varying asymmetrical split-spread geometry within each gather. This method is field-efficient and also yields some files with long shot-receiver offsets of up to 600 m for refraction interpretation.

The P-wave velocities in the Quaternary cover ($V_P = 0.6$ (0.1 km s^{-1}) and the crystalline rocks were obtained from the first

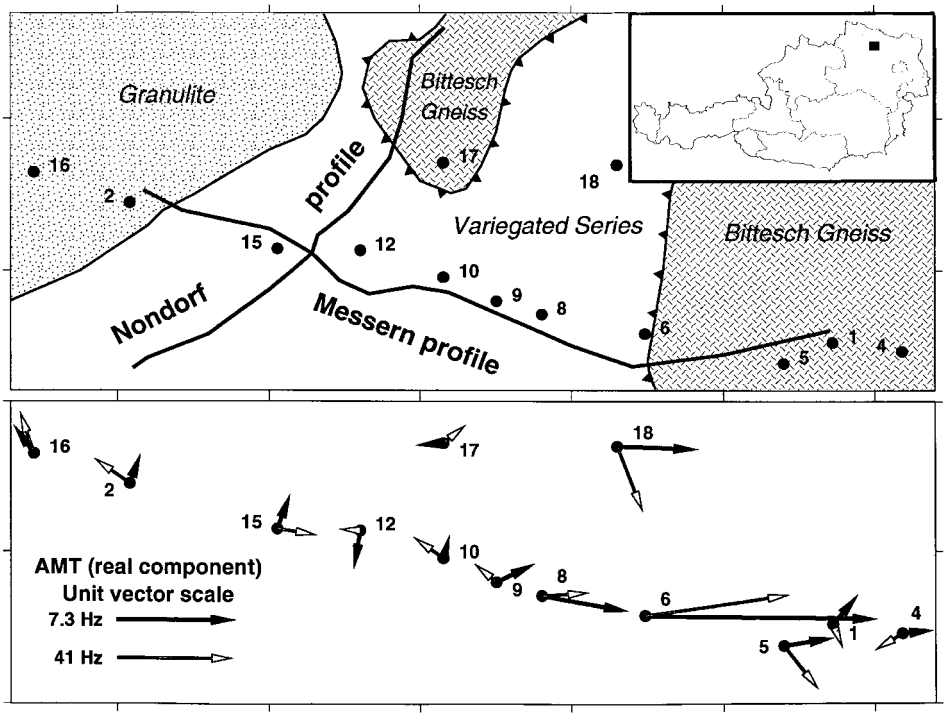

Figure 1 Top: Location map of the seismic profiles (full lines), magnetotelluric (MT) and audio-magnetotelluric (AMT) sites (numbers with black dots), superimposed on the solid geology (simplified from Geologische Bundesanstalt 1984). Inset shows location of detailed map (black square) in Austria. The Variegated Series comprises marble, quarzite, paragneiss (sometimes with graphite or amphibolite), mica schist, and granitic gneiss. The Bittesch Gneiss–Variegated Series boundary is a tectonic contact (direction of teeth symbols indicates dip). Bottom: Real components of the induction vectors at two frequencies, 7.3 and 41 Hz. Tick marks round edge of each map are at 1 km interval.

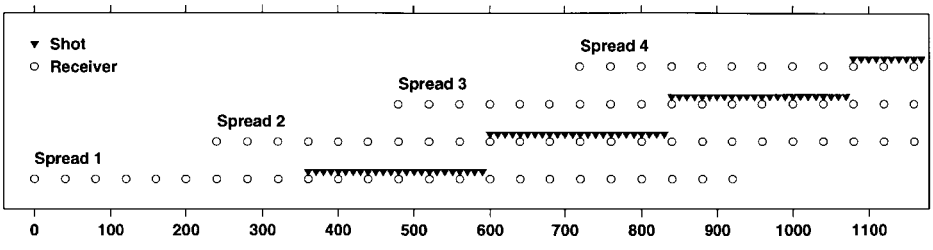

Figure 2 Seismic acquisition geometry showing a 24-channel spread shifted to the right by 6 channels (successive positions 1–4). Scale along bottom is in metres. Receiver spacing is 40 m. The shot point moves along the profile at a constant 10 m interval, giving 24 shots for each spread. Each receiver therefore records data from $4 \times 24 = 96$ shots. The data are sorted first as 96-fold common receiver gathers, then into 12-fold CMP gathers at a 5 m CMP interval.

arrival travel times using the generalized reciprocal method developed by Palmer (1981). Due to the length of the seismic profiles and the relatively small energy of the weight drop, useful seismic refraction information is confined to the uppermost 100 m of the bedrock. The most significant result (Fig. 3) is a remarkable V_P contrast between the Bittesch Gneiss (5.4 ± 0.2 km s^{-1}) and the Variegated Sequence (4.6 ± 0.2 km s^{-1}). Local variations of V_P are a second-order effect in comparison to the marked velocity contrast of these two units.

Static corrections were derived from the refraction seismic results for the reflection processing. Datum was 540 m above mean sea level. A bandpass filter (60–130 Hz) and a 50 Hz notch filter were applied to the CMP gathers, the latter to remove the mains pickup affecting mainly the eastern end of the profile. A set of constant velocity brute stacks was produced. Based on these, a final brute stack with a constant 5.5 km s^{-1} stacking velocity for the topmost 100 ms, with 6.0 km s^{-1} beneath, gave the best results (Fig. 4, top).

The processing had to be performed with caution because of the expected steep inclination of reflecting elements. The topmost 100 ms of the section is very sensitive to the chosen stacking velocity and to the static corrections applied. At greater depth the assumed velocity is less critical. NMO-corrected gathers were inspected to see whether there was any influence of first breaks or later refracted events (stacking in of refracted events as reflections is the commonest pitfall in shallow reflection processing). A 30–50% stretch mute was tried, the latter being preferred. This mutes out the early portion of any traces which have been NMO-stretched, and

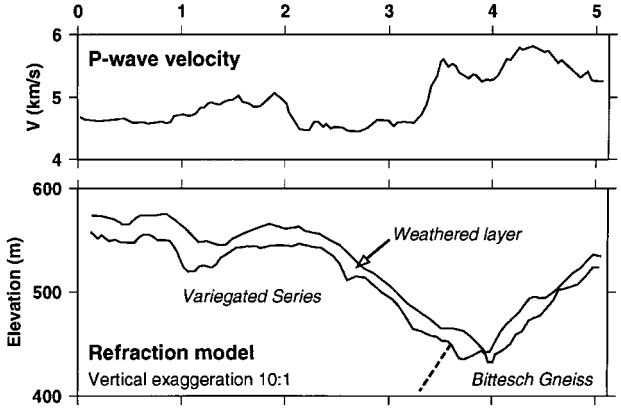

Figure 3 Refraction interpretation of the Messern seismic profile, showing topography (elevation above sea-level), thickness of Quaternary sediments, and P-wave velocity of the crystalline rocks. Horizontal scale is distance along profile in kilometres from the western end.

also offers a way of removing first breaks automatically. In addition, a compromise single front-end mute was applied to ensure that first breaks were completely removed.

The resulting brute stack (Fig. 4) shows real events to a depth of 440 ms at the western end. The very shallow W-dipping events between 2 and 3 km along the profile were double checked by inspection of the CMP gathers to confirm that they are indeed reflected events.

The finite difference depth migration (45° algorithm), using a constant velocity of 5.5 km s^{-1} (Fig. 4, bottom), shows some good reflectors dipping smoothly to the west from 0.4 to 0.6 km and from 1.1 km to 1.2 km depth in the middle of the section. A Stolt FK migration with a constant 5.5 km s^{-1} migration velocity was carried out (not shown here) with results comparable to those shown in Fig.4.

Magnetotelluric and audiomagnetotelluric soundings

Acquisition

These methods help to define the subsurface electrical properties such as resistivity, which is an important parameter for the geological interpretation of the profiles (e.g. Cagniard 1953). They use the local deformations of natural electromagnetic fields of long periods $T > 1$ s (MT) and short periods $T < 1$ s (AMT). The geoelectric layer structure of the

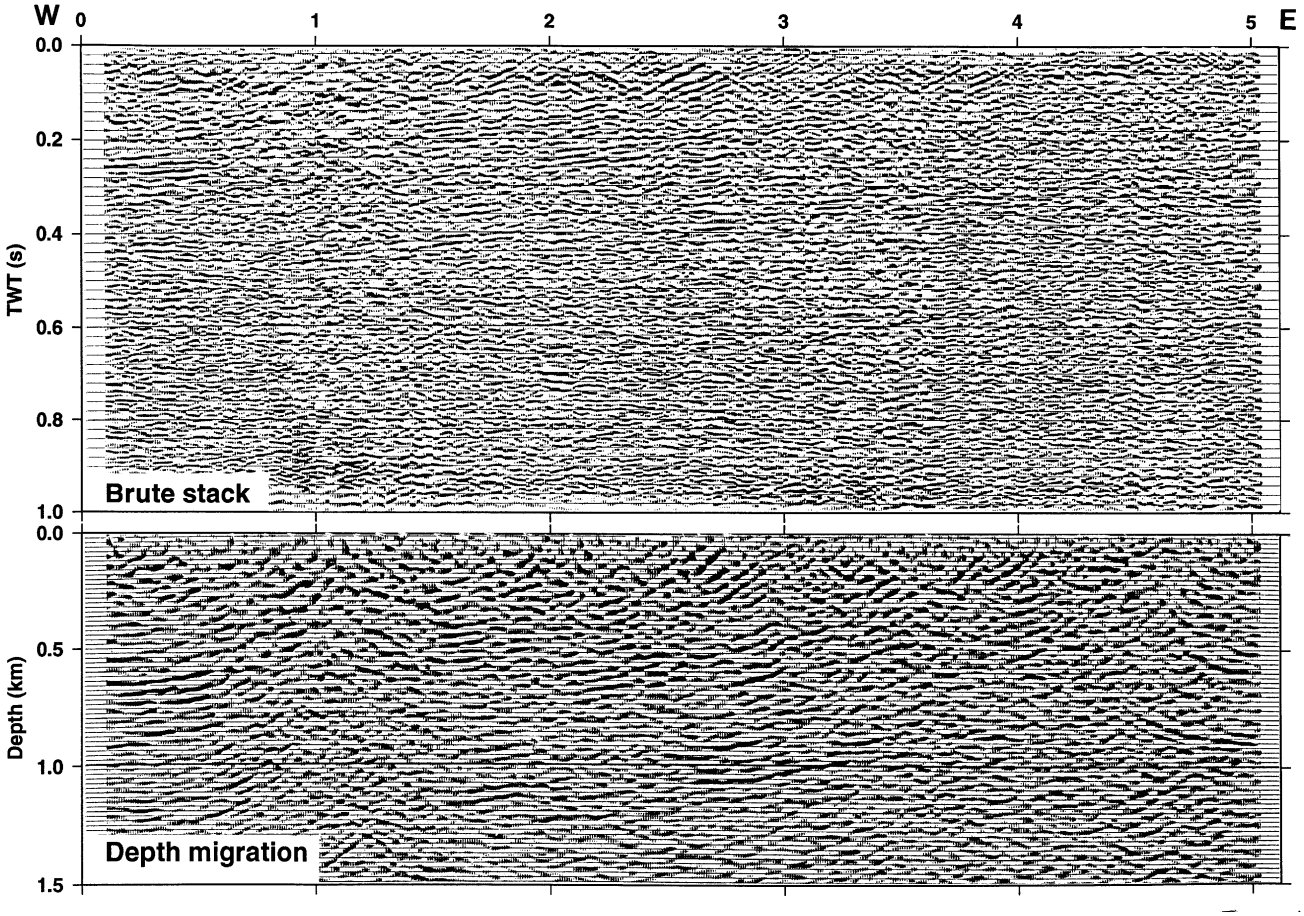

Figure 4 Seismic reflection sections of the Messern profile. Distance along profile in kilometres shown along top. Top: Brute stack (TWT – two-way-travel time in seconds). Bottom: Finite difference depth migration using a constant migration velocity of 5500 m s^{-1} (vertical scale = horizontal scale). Resistivity stations 1 and 2 are approximately at the right-hand and left-hand ends of the profile, respectively.

subsurface can be determined by these methods. The MT and AMT measurements were carried out at 12 sites located along the Messern profile (Fig. 1). In addition to these methods, the ratio of the variations of the vertical to horizontal magnetic components (i.e. the induction vector) permits a general test of the lateral variations of the electrical resistivity. The real component of the induction vector, calculated from the AMT measurements (in our case at constant frequencies of 7.3 and 41 Hz; Fig. 1) is generally directed towards the area of lower electrical resistivity (Parkinson 1962). This effect is not so clear in complicated structures. The length of the vector is proportional to the variation of the ratio of the vertical to the horizontal components of the magnetic field, which theoretically should vanish in horizontally layered media. Therefore, the vector acts as an indicator of lateral inhomogeneities of the electrical parameters. Figure 1 (bottom) shows a great change in the induction vectors at the contact zone between the electrically different Bittesch Gneiss and Variegated Sequence. There is a rotation of 90° or more in the direction of the vector between sites 8 and 9, as well as between sites 17 and 18, and furthermore the lengths of the vectors are drastically reduced. This is a further example of the phenomenon which has been observed in many cases (for example by Arora & Adam 1992), that inside the conductor these strongly reduced-amplitude vectors point in the strike direction, probably due to 3-D effects inside the conductor.

1D inversion

Since site 1 (Messern) in the Bittesch Gneiss and site 2 (Rotweinsdorf) in the Granulite are nearly undisturbed, a standard program of 1D inversion (Steiner 1989) of the AMT and MT data at each site was applied to their extreme sounding curves (ρ_{max} and ρ_{min}), expressing the strong anisotropy of the metamorphic rocks. The resulting distribution of electrical resistivity is shown in Table 1,

Table 1: Results of 1D MT and AMT inversions at sites 1 and 2. Layer thickness *T* and depth to base *D* in metres; log (ρ_{max}), log (ρ_{min}): $\log_{10}$ of maximum and minimum resistivity, in Ω m. Figures have been rounded to the appropriate level of significance.

Site 2 (Rotweinsdorf)			Site 1 (Messern)		
T	*D*	log (ρ_{min})	*T*	*D*	log (ρ_{min})
400	400	0.95	3	3	0.60
670	1100	0.30	1300	1300	5.08
2200	3300	−1.00	3900	5200	1.08
–		> 4	—		> 4
T	*D*	log (ρ_{max})	*T*	*D*	log (ρ_{max})
7	7	0.30	8	8	1.11
270	270	3.51	1100	1100	4.49
1700	2000	1.18	14000	15000	2.96
—		3.00	—		> 4

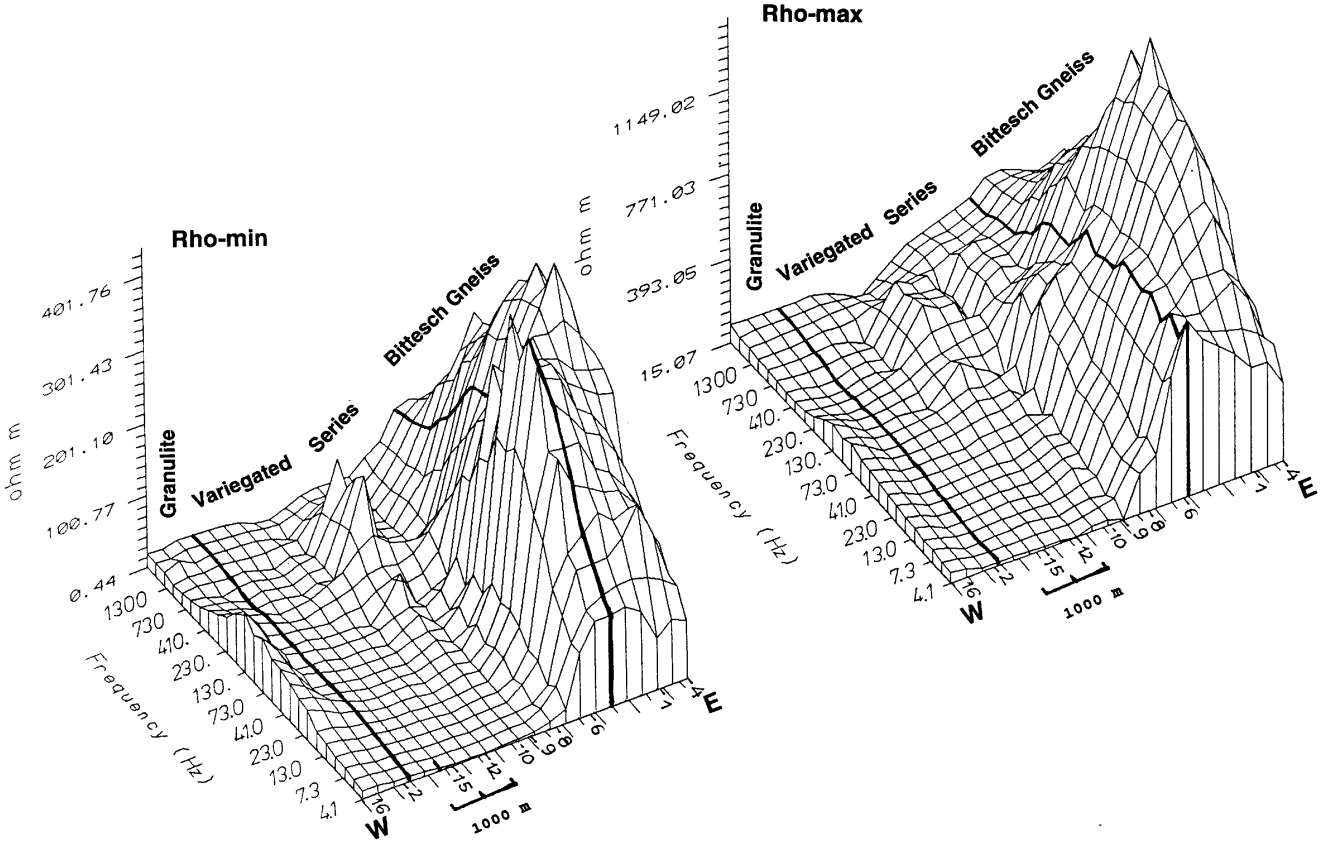

Figure 5 Distribution of ρ_{min} [rho-min] and ρ_{max} [rho-max] as a function of distance along the Messern profile and frequency (Hz). Numbers show locations of the AMT sites (Fig. 1). Note that the vertical scales are different. The surface boundaries of the three principal rock groups are shown by the bold lines.

in which the maximum and minimum resistivity ρ_{max} and ρ_{min} are functions of depth only. This modelling supplies some general trends in the electrical resistivity. Three important results can be emphasized:

- In the western part of the profile both ρ_{max} and ρ_{min} are much lower than expected for dry crystalline rocks.
- Both ρ_{max} and ρ_{min} in the uppermost 1000 m are very much lower below site 2 than below site 1.
- There is some evidence of a high conductivity layer at a few hundred metres depth below the western part of the profile.

The large difference between ρ_{max} and ρ_{min} indicates strong anisotropy, as would be expected in metamorphic rocks with graphitic or pyrite mineralization (e.g. Adam 1987; Adam *et al.* 1990). In our study area lateral resistivity variations are significant as well, but these may be due to tectonic or other effects. Similar graphitic conductors have been indicated and studied in detail at the deep borehole KTB in Oberpfalz, Germany, which is located at the western edge of the Bohemian Massif. Here graphite (or carbon) has accumulated along shear zones (ELEKTRB-Gruppe Windischeschenbach 1984).

2D inversion

Figure 5 shows ρ_{min} and ρ_{max} as functions of the location and frequency, presenting both lateral variations and the frequency dependency of the parameters. The latter can be regarded as a very rough reciprocal value of the depth range from which the information is relevant. They show a complex lateral distribution. A 2D inversion has also been carried out (Fig. 6).

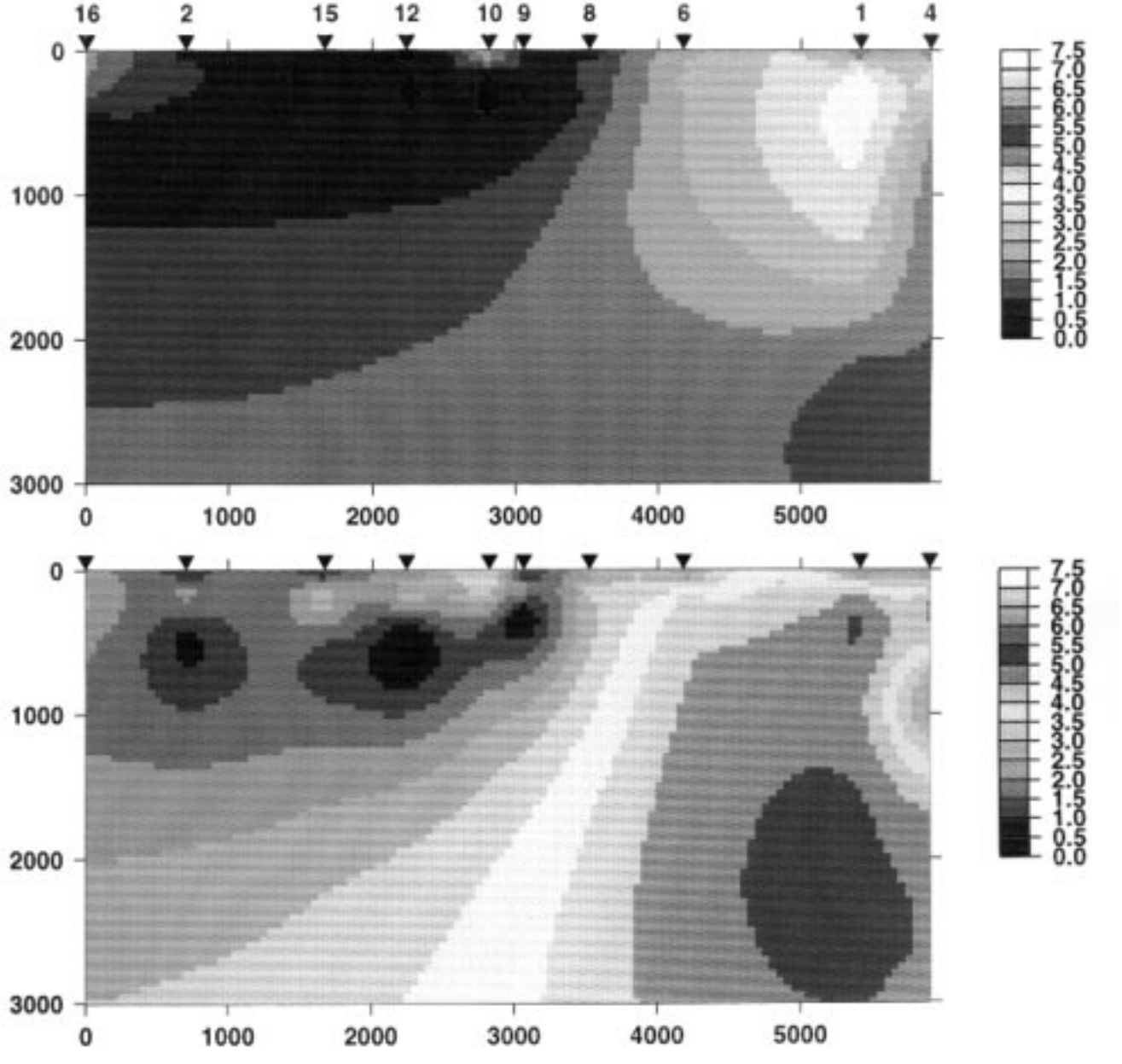

Figure 6 Two dimensional resistivity models of the Messern profile (distance and depth in metres). Top: log (ρ_{min}). Bottom: log (ρ_{max}).

The modelling confirms that the highly conducting layer should be interpreted as the Variegated Sequence. At the surface this formation is cut by the Bittesch Gneiss at approximately site 6 (Fig. 1).

The 2D inversion (Fig. 6) shows that the electrical structure is strongly 2D, so this inversion is to be preferred to the separate 1-D inversions discussed above. There is a highly conductive zone in the western half of the profile with a thickness in the range of 600–1000 m, at distances from 1200 m to 3000 m along the profile. The resistivities are around ρ_{max} = 30 Ωm and ρ_{min} = 3 Ωm. This zone is interpreted as the Variegated Sequence. Between sites 2 and 8 outcropping graphite and/or pyritic accumulations are expected (Fuchs & Matura 1980; Schrauder *et al.* 1993). The zone of low conductivity in the eastern half of the profile is due to the Bittesch Gneiss, which dips west under the Variegated Sequence (log $\rho_{max} \geqslant$ 2.5–3.5; log $\rho_{min} \geqslant$ 1.5). At the western end of the profile, between points 0 and 900 m, there is evidence of a contrast between the Granulite and the Variegated Sequence, with $\rho_{max} \approx$ 100 Ωm and $\rho_{min} \approx$ 10 Ωm in the Granulite.

Combined interpretation of seismic, MT and AMT measurements

The results of both AMT and seismic measurements correlate with geological and tectonic features in the Rotweinsdorf-Messern area. Because of the different accuracy and physical significance of the seismic and the AMT models a joint interpretation can be proposed, but with some reservations. Figure 7 shows our preferred interpretation of the Messern AMT, MT and seismic profiles, based on the data shown in Figs 3–6.

Bold solid lines are seismic reflector segments interpreted from Fig. 4 and projected onto this profile. We have not interpreted any reflectors on the depth migration which do not have clear counterparts on the stack. The very shallow W-dipping events at 2–3 km along the seismic profile are not stacked-in refractions, although the stack shows that the events are of relatively low frequency due to NMO stretch. However, other very shallow events, whether dipping west or east, have been omitted from interpretation, as they may be artefacts. The E-dipping reflector at 0.3 km depth, 1.2 km distance on the seismic profile, may be side-swipe, or else is an artefact of the low signal to noise zone at around 1 km distance on the seismic data (Fig.4). The strong events at 0.5–0.8 km depth at the very western edge of the reflection data are not migration edge artefacts, as they are clear on the stack. All the interpreted real reflectors therefore dip to the west, with the dip shallowing out both westwards and downwards.

There is no seismic reflection or refraction information on the Granulite – Variegated Series boundary. The inferred boundary (dashed line in Fig. 7) is based on the lower conductivity of the Granulite relative to the very conductive Variegated Series (Fig. 5). The Variegated Series appears to be characterized by very high conductivity and relatively good reflectivity. We identify the base of the series by tracing it down-dip to the west through a zone of reflectors, and flattening out below about 1 km depth on the basis of the 2-D resistivity modelling (Fig. 6). In part, the high reflectivity at the base of the Variegated Sequence may be due to the V_P contrast (4.5–5.5 km s^{-1}) between it and the Bittesch Gneiss. The local absence of reflectors below 0.5 km depth in the region below MT site 15 (Fig. 7) is probably due to the above-mentioned noisy zone.

In our interpretation the flat-lying deep reflectors below about 1 km depth in the middle of the profile (Fig. 7) lie within the Bittesch Gneiss, but we do not have enough information to interpret them further.

Conclusions

The boundary between Moldanubian (the Dobra Gneiss, overlain by granulites) and the Moravian (Bittesch Gneiss) is separated by the Variegated Sequence. Two different tectonic hypotheses have been proposed. One model suggests a link of the Bittesch Gneiss to the Dobra Gneiss by a synclinorial (trough-shaped) structure. The other model involves concordant overthrusting to the east of Moravian formations by the Moldanubian. Our spatially very limited data are consistent

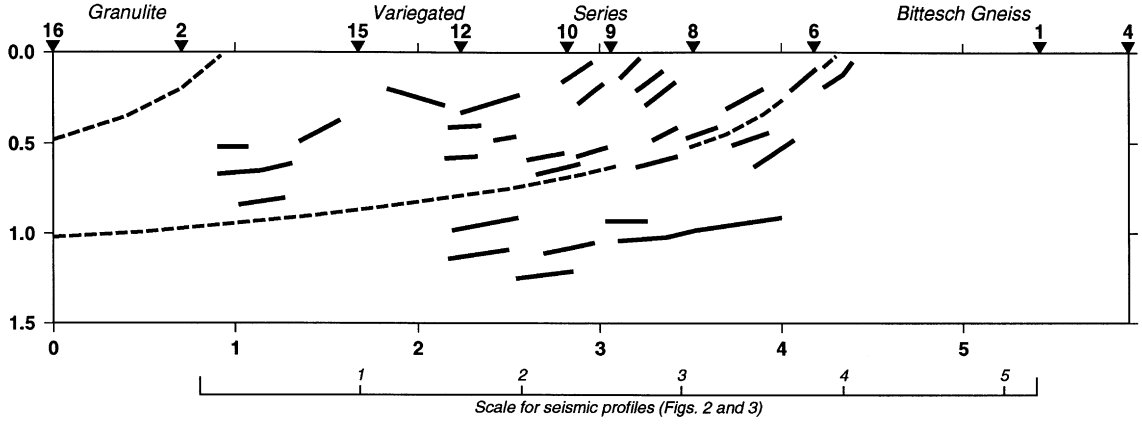

Figure 7 Preferred interpretation of Messern AMT, MT and seismic profiles. Bold solid lines are seismic reflector segments interpreted from Fig. 4 and projected onto this profile. Extent of the Messern seismic profile is indicated beneath. Dashed lines are interpreted boundaries of the top and bottom of the Variegated Series.

with either model. Although we have not been able to discriminate between the models, this result confirms that the modest resources of engineering scale geophysical techniques can be used to image structures within crystalline basement down to depths of about 1 km.

Acknowledgements

This study is part of the *Pre-Alpine Crust in Austria, S-47 Geo* project, sponsored by the Fonds zur Förderung der Wissenschaftlichen Forschung in Österreich (FWF) project no. S 4701. Some of the diagrams were prepared using the public-domain GMT system (Wessel & Smith 1991).

References

Ádám, A. [1987] Tectonic effects in magnetotelluric field and their numerical modelling. *Gerl. Beitr. Geophys.* **96**, 17–31.

Ádám, A., Duma, G. and Horvath, J. [1990] A new approach to the electrical conductivity anomalies in the Drauzug-Bakony geological unit. *Phys. Earth Planet. Int.* **60**, 155–162.

Arora, B.R., Adam, A. [1992] Anomalous direction behaviour or induction vectors above elongated conductive structures and its possible causes. *Phys. Earth Planet. Int.* **74**, 183–90.

Brückl, E. [1988] A seismic system for shallow-depth investigations, Poster presented at the *50th EAEG meeting, 610 June 1988, The Hague, Netherlands*, and unpublished reprint.

Cagniard, L. [1953] Basic theory of the magnetotelluric method of geophysical prospecting. *Geophysics* **18**, 605–35.

ELEKTRB—Gruppe Windischeschenbach [1984] Untersuchengen zur elektrischen Leitfähigkeit in der kontinentalen Tiefbohrung und ihrem Umfeld-Was bringen sie uns Neues? *Deutshes Geophys. Gesell. Mitt.* **4**, 240.

Fuchs, G. and Matura, A. [1980] Die Böhmische Masse in Österreich. In: *Der Geologische Aufbau Österreichs*, pp. 121–143. Springer, Vienna.

Geologische Bundesanstalt [1984] Geologische Karte der Republik Österreich 1: 50,000, Sheet 20 (Gföhl), Vienna.

Nagy, Z. [1996] Advances in the combined interpretation of seismics with magnetotellurics. *Geophys. Prospect.* **44**, 1041–1083.

Palmer, D. [1981] The generalized reciprocal method of seismic refraction interpretation. *Geophysics* **46**, 1508–18.

Parkinson, W.D. [1962] The influence of continents and oceans on the geomagnetic variations. *Geophys. J. R. astr. Soc.* **6**, 441–9.

Schrauder, M., Beran, A., Förness, S. and Richter, W. [1993] Constraints on the origin and the genesis of graphite bearing rocks of the variegated sequence of the Bohemian Massif. *Miner. Petrol.* **49**, 175–88.

Steiner, T. [1989] MT inversion using least-absolute-values and least squares. *Abstracts and Papers of the Technical Program. 34. Geophysical Symposium, Budapest, 4–8 September, 1989, pp.* 639–651.

Thiele, O. [1976] Ein westvergenter kaledonischer Deckenbau im niederösterreichischen Waldviertel. *Jb. Geol. Bundes. Öst.* **119**, 75–83.

Wessel, P. and Smith, W.H.F. [1991] Free software helps map and display data. *Eos Trans. Am. Geophys. Un.* **72**, 441.

Wieseneder, H., Freilinger, G., Kittler, G. and Tsambourakis, G. [1976] Der kristalline Untergrund der Nordalpen in Österreich. *Geol. Rndsch.* **65**, 512–25.

MS submitted January 1997, revised April 1997, accepted May 1997